A novel Turkish natural zeolite (clinoptilolite) treated with hydrogen peroxide for Ni 2+ ions removal from aqueous solutions

Article *in* Desalination and Water Treatment · February 2015

DOI: 10.1080/19443994.2015.1011707

2 authors:

Murat canlı
Ahi Evran Üniversitesi

Yüksel Abalı
Manisa Celal Bayar University

Taylor & Francis
Taylor & Francis Group

Desalination and Water Treatment

ISSN: 1944-3994 (Print) 1944-3986 (Online) Journal homepage: http://www.tandfonline.com/loi/tdwt20

A novel Turkish natural zeolite (clinoptilolite) treated with hydrogen peroxide for Ni^{2+} ions removal from aqueous solutions

Murat Çanli & Yuksel Abali

To cite this article: Murat Çanli & Yuksel Abali (2015): A novel Turkish natural zeolite (clinoptilolite) treated with hydrogen peroxide for Ni^{2+} ions removal from aqueous solutions, Desalination and Water Treatment, DOI: 10.1080/19443994.2015.1011707

To link to this article: http://dx.doi.org/10.1080/19443994.2015.1011707

Desalination and Water Treatment
www.deswater.com
doi: 10.1080/19443994.2015.1011707

(2015) 1–11

Taylor & Francis
Taylor & Francis Group

A novel Turkish natural zeolite (clinoptilolite) treated with hydrogen peroxide for Ni^{2+} ions removal from aqueous solutions

Murat Çanli[a,*], Yuksel Abali[b]

[a] *Department of Primary School, College of Education, Celal Bayar University, Demirci/Manisa 45900, Turkey, Tel. +90 5062861600; Fax: +90 2364621600; email: murcanli@yahoo.com*
[b] *Department of Chemistry, College of Arts and Sciences, Celal Bayar University, Manisa 45100, Turkey, Tel. +90 2362013154; Fax: +90 2362412158; email: yabali@yahoo.com*

Received 26 May 2014; Accepted 15 January 2015

ABSTRACT

The removal of Ni(II) from aqueous solution by batch adsorption technique using a novel Turkish zeolite from Akdere region was investigated. Activation of the zeolite was achieved with hydrogen peroxide. After elementary characterization of the adsorbent, the influence of contact time, pH, adsorbent amount, initial Ni(II) concentration, and temperature on the selectivity of the removal process was investigated. Results showed that increase in adsorbent dosage led to increase in Ni(II) adsorption due to increased number of adsorption sites. Freundlich model fitted the experimental data better than Langmuir model. Adsorption process was found to be highly pH dependent. The optimum pH for adsorption of Ni(II) was found to be 7. Adsorption equilibrium attained within 1 h time. The sorption of Ni(II) increased with rise of temperature. The adsorption process was spontaneous (ΔG° ads <0) and endothermic (ΔH° ads >0), supporting also the chemisorption is the rate-determining step.

Keywords: Ni(II) removal; Zeolite; Isotherms; Kinetics; Thermodynamic values

1. Introduction

Heavy metals such as nickel, cobalt, and iron are widely used in several industrial activities. Nickel is especially the main material in plating and cadmium–nickel battery, phosphate fertilizers, mining, pigments, stabilizers, and alloys. Throughout wastewater discharge, nickel finds its way to the aquatic environment as pollutants. The amount of nickel is significantly increased in plants by absorbing it from wastewaters. By consuming those types of plants in great amounts nickel can cause kidney and liver failure, and some types of cancer. Because of their high toxicity to the environment, it is a major issue to remove heavy metals from industrial wastewaters [1,2].

There are already several methods in use for removal of heavy metals such as chemical precipitation, membrane separation, ion exchange, evaporation, and electrolysis. However, they have high cost and are not effective for dilute solutions [3,4]. Adsorption shows high selectivity for a certain metal, even in small concentrations, that is the main reason for its preference over other methods [5,6]. In this scenario, the limit value for charging nickel to electroplating industry wastewater is 0.5 mg/L.

---

*Corresponding author.

The choice of adsorbents in removal process has great influence on affectivity of adsorption. In this manner, natural zeolite that is a common resource of aluminosilicates seems becoming an alternative with being available all over the world [6,7]. Clinoptilolite, one of the most common natural zeolites, is a hydrated alumina–silicate member of the heulandites group occurring in the zeolitic volcanic tuffs. Clinoptilolite is characterized by connected infinite three-dimensional frameworks of $[AlO_4]^{5-}$and $[SiO_4]^{4-}$. This tetrahedral linked to each other like honeycomb by sharing all of the oxygens, and the negative charge being balanced by metal cations, like Na^+, K^+, Ca^{2+}, and Mg^{2+}. Metal ions are trapped by clinoptilolite with ion-exchange of those metal cations [8].

The adsorption capacity of natural zeolites is raised to higher levels using several methods such as acid and thermal activation and modification by metal oxides or any other groups [9–12]. The main purpose of using acid in activation is to create a medium in which metal cations in the structure of zeolite are removed; and thus, zeolite structure get more spaces in the honeycomb chain for adsorption. Strong acids like hydrogen chloride and sulfuric acid are commonly used in acid activation of clay materials [13,14]. A relatively weaker acid which is hydrogen peroxide is preferred in this study.

The zeolite as an adsorbent mainly composed of clinoptilolite was used due to its low cost and high efficiency. The main factors influencing the adsorption capacity of the composite such as the initial pH value of the metal ions solutions, contact time, the initial concentration of metal ions solutions, and temperature were investigated. In order to examine the controlling mechanism of the adsorption process, the kinetics, adsorption isotherms, and thermodynamics parameters were evaluated.

2. Materials and methods

2.1. Materials

The natural zeolite (clinoptilolite) sample comes from volcanic tuffs cropped out in Akdere region (City of Manisa, Turkey), and has the following elemental composition: $(NaKCa_{0.5})_{5.4}(Al_{5.4}Si_{30.6}O_{72})\cdot 20H_2O$ ($Si/Al = 5.21$). The zeolitic volcanic tuff was used as collected. $NiCl_2\cdot 6H_2O$ (from Merck) were used as metal ion source for the adsorption experiments. All the reagents were of analytical grade or highest purity available and used without further purification. H_2O_2 solution with 50% has been preferred to activate zeolite.

2.2. Adsorption studies

Metal ion retention properties of the zeolite samples were carried out using a batch equilibrium procedure. Thus, 0.1 g of dried zeolite was placed in a flask and contacted with 100 ml of the aqueous solution of Ni^{2+} ion at different temperatures and pH [15]. The kinetics of the metal ion retention was studied by placing 0.1 g of dried zeolite in 100 ml of aqueous solution of metal ion with a concentration of 20 mg/L at 25°C, the equilibrium concentration of the metal being measured at different contact times ranging between 15 and 240 min. The effect of medium pH on the adsorption capacity of the zeolite was investigated in the pH range 2.0–9.0 at 25°C. To determine the effect of initial concentrations of the metal ion on the adsorption rate and capacity on the zeolite, the initial concentration of the Ni^{2+} metal ion solutions was varied between 10 and 100 mg/L in the adsorption medium at pH 7.0.

The zeolite was filtered off, and the residual concentration of Ni^{2+} remained in the filtrate was measured by the atomic absorption spectrophotometry (AAS) spectroscopy. AAS spectroscopy was performed on a Varian SpectrAA 220 (Varian Inc., Palo Alto, Germany). The amount of metal ion bound on the zeolite was calculated by following equation:

$$q_e = \frac{(C_0 - C_e)V}{m} \tag{1}$$

where C_0 and C_e are the initial and equilibrium concentrations (mg/L) of metal ion in solution, respectively; V the volume (L); and m is the weight (g) of the adsorbent.

2.3. Method validation and Q_A/Q_C

For each adsorption experiments four replicates were performed. Analytical precision was assessed by means of four replicate analyses of 500 ml of Ni^{2+} stock solution. Multiple reference solutions and blank solutions were administered. The calibration graphs were prepared on the different days and the calibration equations were checked. After stabilizing the equation of calibration, some of the standards were read repeatedly and their concentrations were calculated. The percent relative error was always less than 5%. The r^2 values for calibration plots were greater than 0.99.

3. Results and discussion

3.1. Characterization of natural zeolite

Roof vibrations of zeolites at remote IR and mid-IR regions give typical peaks (Fig. 1). 1,200–300 cm^{-1} region is called structural fingerprints for zeolites [16]. 3,630, 1,630, 1,200, 1,055, 673, and 607 cm^{-1} are characteristic peaks for clinoptilolite [17]. In this study, the inner tetrahedra making asymmetric stretching gave a peak at the 1,050 cm^{-1} as required in the range of 1,250–920 cm^{-1}. Likewise, the sample gave a symmetric stress peak at 713 cm^{-1} as it is expected to be in the range of 720–650 cm^{-1}. Al–O vibration peak was observed at 460 cm^{-1} as it should be seen in 500–420 cm^{-1}. For natural zeolites, while absorption occurs in the region 1,250–660 cm^{-1}, due to adsorbed water, a characteristic peak is observed deformation at 1,640 cm^{-1}. Ünaldı et al. [17] found these stresses and vibrations at the peaks of 469.521, 607, 637, 746, 795, 1,502, 1,638, 3,463, and 3,629 cm^{-1}.

SEM images pointed out that hydrogen peroxide formed decomposition on zeolite surface (Fig. 2(b)) while gaps resulting in the structure are observed with acid activation (Fig. 2(c)). Acid and peroxide cause broken structural bonds of zeolite which become more porous [18]. Fig. 2(d) and (a) which are modified with metal ions in the structure indicates that the gaps filled.

Chemical composition of zeolite was found in different studies as follows (Table 1), Jha and Hayashi [19] % 77.96, 14.02, 1.30, 1.15, 3.88, 1.23, and 0.46, for Taffarel and Rubio [20] % 72.26, 12.42, 5.88, 0.34, 1.06, 6.19, 0.52, and in another study [21] it was % 70.90, 10.49, 1.35, <0.2, 3.58, 2.82, 0.92. The zeolite in this study is a clinoptilolite type of zeolite because the Si/Al ratio is 4.6 [22]. The structure of the zeolite was determined with XRD (Fig. 3). The peaks at the XRD graph points out a sharp and perfect crystallization and also proves that this is an almost pure clinoptilolite. All peaks are formed in $a = 7.41$ Å, $b = 17.89$ Å, $c = 15.85$ Å, and $\beta = 91°29'$ which point out a monoclinic system within the structure of $(Na, K)_6(Al_6Si_{30}O_{72})20H_2O$ [23]. In XRD graph, the peaks at $2\theta = 9.87°$, 22.4°, and 30° prove that the zeolite has clinoptilolite. Yetgin [24] found same peaks belong to clinoptilolite at 9.77°, 22.31°, and 29.96°. In several other studies [25,26], similar results have been pointed for clinoptilolite samples in XRD graphs. Peroxide activation over zeolite has created smaller peaks than natural zeolite on XRD because the structure of clinoptilolite started to lose water and other metal cations like Ca and Mg (Fig. 3).

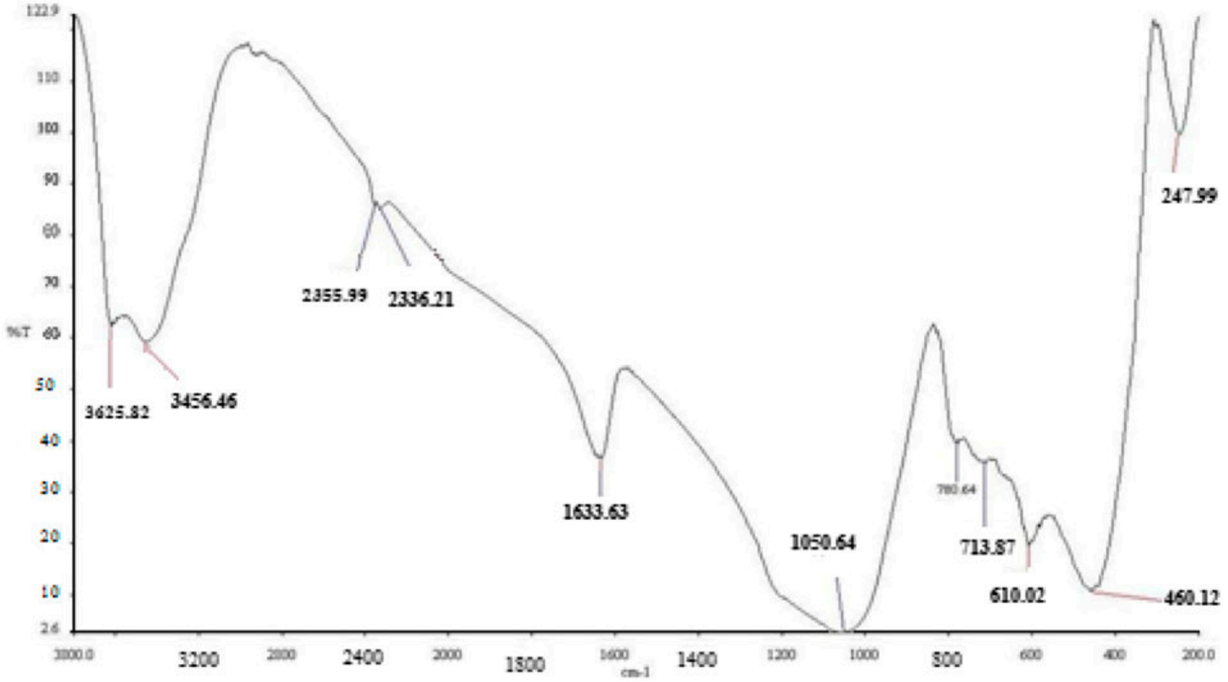

Fig. 1. FTIR graph of Akdere natural zeolite.

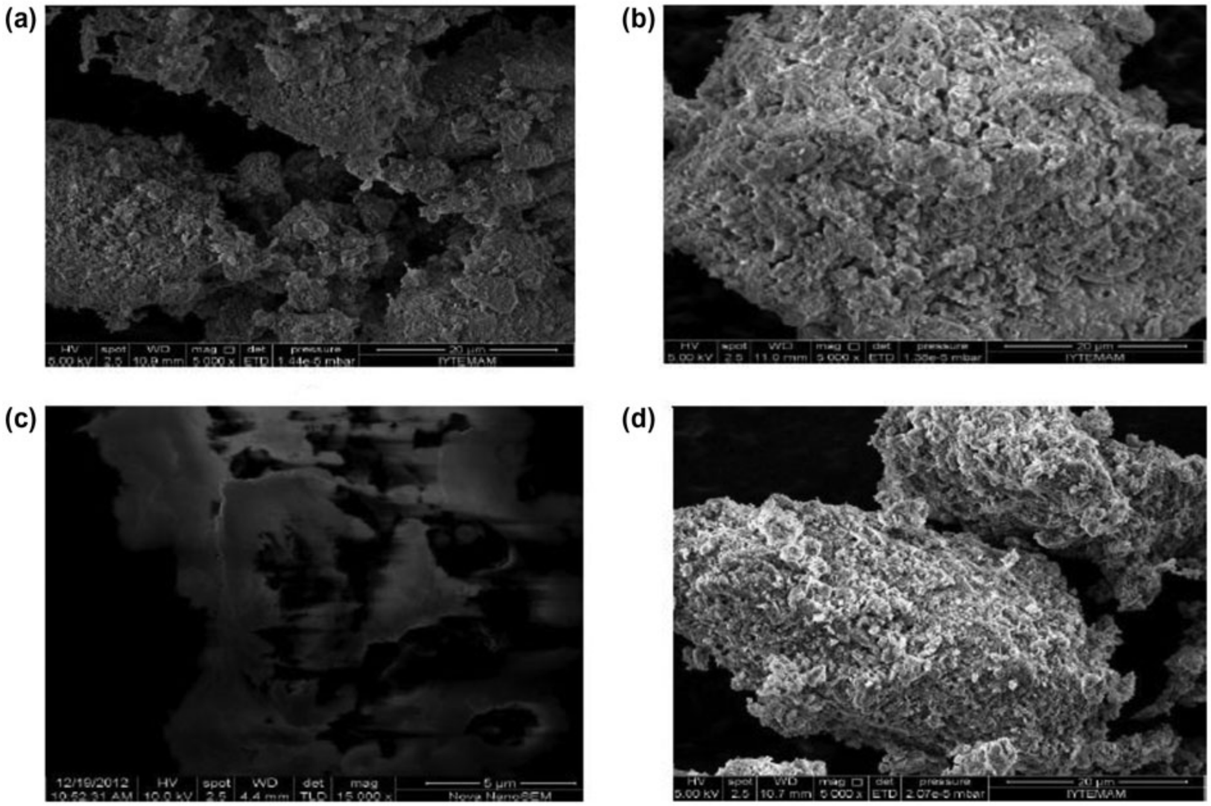

Fig. 2. SEM images of zeolite samples: (a) natural akdere zeolite, (b) zeolite treated with peroxide, (c) zeolite treated with chloric acid, and (d) nickel adsorbed zeolite.

Table 1
Physicochemical properties of several natural zeolites from Anatolia region

Compound	% Akdere zeolite (in this study)	Gördes zeolite [32]	Amasya zeolite [33]	Çankırı-Çorum zeolite [34]	Bigadiç zeolite [35]
SiO_2	73.90	71.98	70.27	64.28	71.81
Al_2O_3	14.17	12.56	12.90	12.07	12.26
Fe_2O_3	1.45	0.45	1.38	0.84	0.80
Na_2O	<0.02	0.92	3.21	5.62	0.50
K_2O	2.94	4.28	1.49	0.83	1.70
CaO	2.99	1.99	2.05	2.47	3.41
MgO	2.47	0.42	1.71	2.07	1.37
Si/Al	**5.21**	**5.73**	**5.44**	**5.32**	**5.85**
Molecular channel size	7.9 × 3.5 Å				
S_{BET}	45.74 m^2/g				
Pore volume	0.11 cm^3/g				
pH	7.9				
Adsorption capacity	3.56 mg/g				

Table 1 presents several properties of Akdere and several other regions' zeolite. The BET surface area and pore volume are 45.74 m^2/g and 0.11 cm^3/g. Having bigger surface area gives zeolite to hold more Ni^{2+} ions on its surface. And also, Akdere zeolite has lower Si/Al ratio than other regions' zeolite sources.

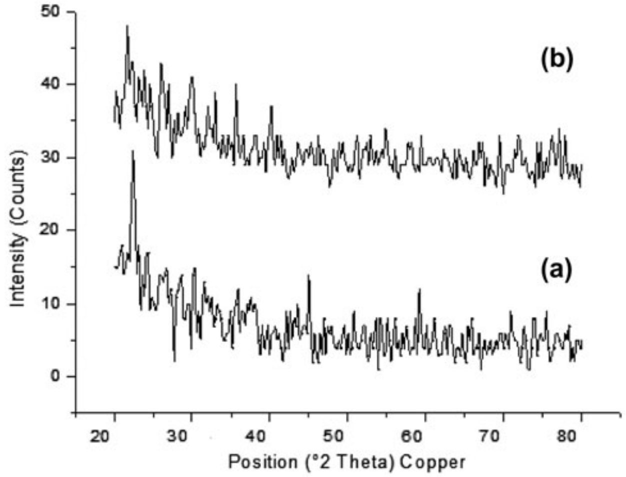

Fig. 3. XRD graph of zeolite: (a) natural zeolite and (b) zeolite treated with H_2O_2.

Having more aluminum content lets the zeolite exchange more cations within its honeycomb structure.

In lights of TG-DTA graph of Akdere zeolite shown in Fig. 3, in order to increase adsorption capacity of the zeolite, zeolitic water was removed without breaking molecular sieves by setting temperature at 250°C for 4 h before using zeolite in adsorption process. The purpose of heating is to get more space in zeolite structure by removing water molecules. Having more spaces and holes on zeolite surface permits more Ni^{2+} ions to get in or hold onto those spaces in zeolite.

For Akdere natural zeolite the pore size distribution only shows one peak centered at 40 Å, suggesting a very narrow pore size. XRD measurement also shows that the natural zeolite is mainly composed of clinoptilolite, quartz, and mordenite [24–26] (see Fig. 4).

3.2. Adsorption and kinetics

The relationship between contact time and adsorbed amount of Ni^{2+} ions was shown in Fig. 5. With increase of contact time, adsorption of Ni^{2+} ions was increased. The equilibrium time was reached at 60 min. Besides, the pH of the metal ion solution plays an important role in the adsorption capacity by the modification of zeolite.

Fig. 6 showed the effect of solution pH on the adsorption capacity of Akdere zeolite for Ni^{2+} ions. The amount of Ni^{2+} adsorbed by Akdere zeolite slowly increased when pH of Ni^{2+} solution increased from 2 to 8, the optimum adsorption pH being located at 7. At low pH, the surface of Akdere zeolite was charged positive, therefore, electrostatic repulsion between Ni^{2+} ions and Akdere zeolite molecules may prevent the adsorption of Ni^{2+} ions onto Akdere zeolite (Fig. 7). The solid slurry of zeolite shows negative charge in aqueous solution if pH is greater than 6. Over 6 for pH values zeolite behaves like an anionic surface.

At pH 6, which is zero point of charge (ZPC) for Akdere zeolite, Ni^{2+} retention was begun to decrease. Over pH 8, huge amount of Ni^{2+} ion started to deposit as $Ni(OH)_2$ because the solution reached to its K_{sp} value (Fig. 8). Between 6 and 8, the maximum adsorption capacity for zeolite was reached. Therefore, the pH of 7 was selected as the initial pH value of Ni^{2+}

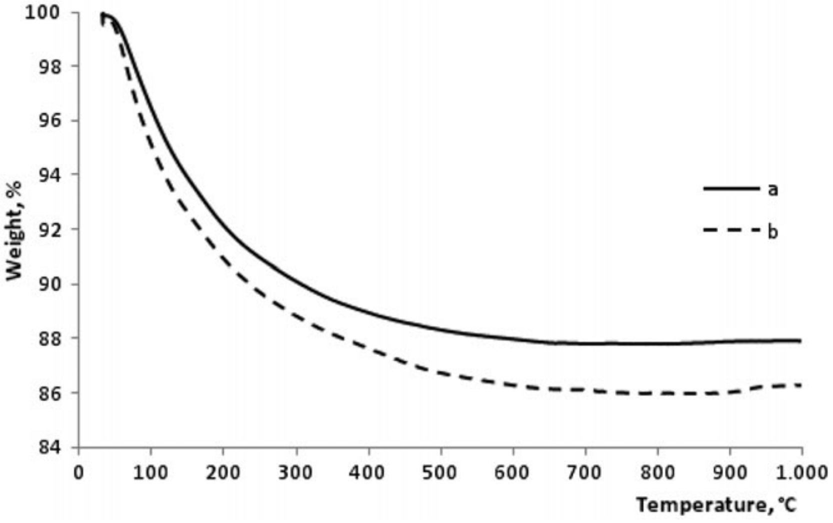

Fig. 4. Thermal analysis of zeolite samples: (a) natural zeolite and (b) zeolite activated with H_2O_2.

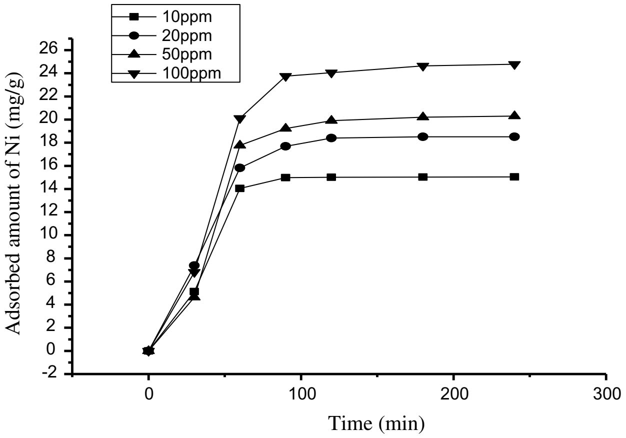

Fig. 5. The effect of contact time on the equilibrium adsorption capacity of Akdere zeolite (adsorbent dosage: 0.4 g/L; contact time: 60 min; and pH 5).

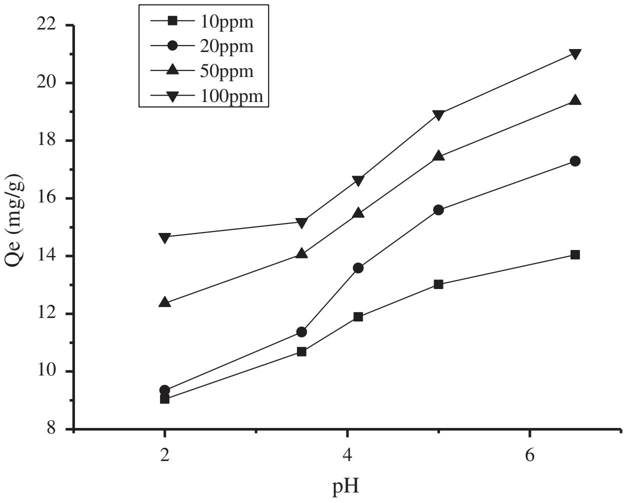

Fig. 6. The effect of pH on the equilibrium adsorption capacity of Akdere zeolite for Ni^{2+} (nickel concentration: 10 mg/L; contact time: 60 min; and 0.4 g/L clinoptilolite).

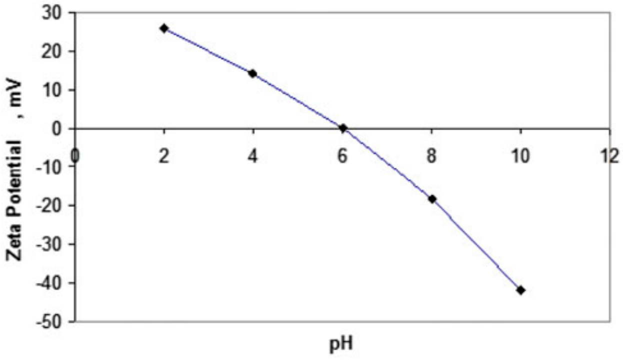

Fig. 7. ZPC on Akdere zeolite.

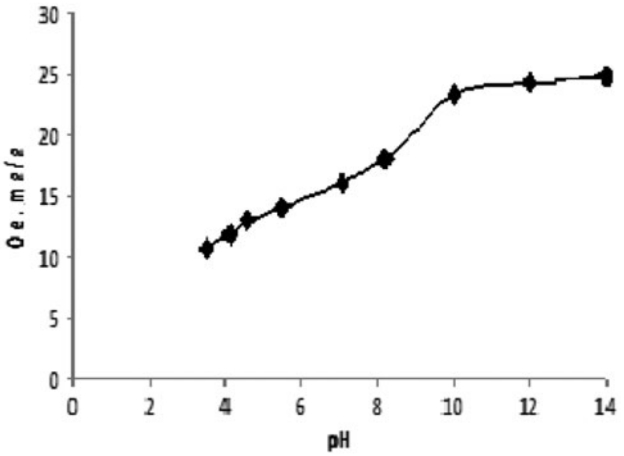

Fig. 8. Effect of whole pH range on Ni adsorption.

solution for the following adsorption experiments. Because of cationic structure of Ni^{2+} ions, natural zeolite can attract more Ni^{2+} ions in alkaline media. The highest increase was happened at 20 mg/L for initial concentration of Ni^{2+} solution.

In adsorption studies, Ni^{2+} with concentration of 20 mg/L and 0.1 g of zeolite was mixed at pH 7 for different time periods with mixing rate of 200 rpm.

Fig. 9 illustrates the dynamic adsorption of Ni^{2+} on Akdere zeolite at different temperatures. The adsorption of Ni^{2+} on the zeolite reached to end at over 20 h (was not shown in the figure). At each temperature, zeolite exhibits high adsorption for Ni^{2+} because of its molecular size. As it can be seen from Fig. 9, adsorption temperature has small influence the adsorption capacity. For the adsorption, the process is usually a

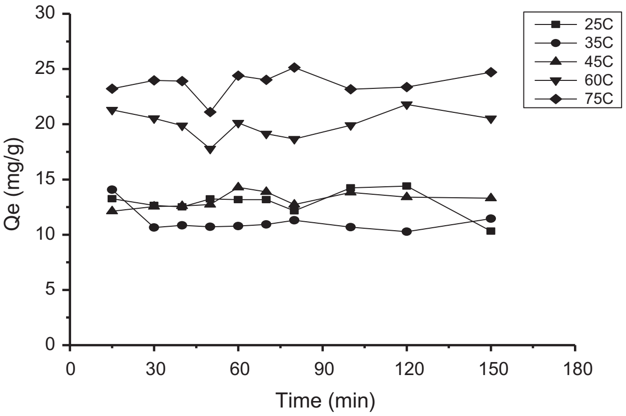

Fig. 9. The effect of temperature on the equilibrium adsorption capacity of Akdere zeolite for Ni(II) ions (nickel concentration: 10 mg/L; contact time: 60 min; 0.4 g/L clinoptilolite; and pH 5).

diffusion process with endothermic property. A higher temperature can result in an increase in the mobility of the Ni^{2+} ions and their energy to undergo an interaction with active sites at the surface of adsorbents. Furthermore, increasing temperature may produce a swelling effect within the internal structure of the zeolite enabling large ions to penetrate further into the pores [27].

The adsorption of charged Ni^{2+} ions onto the adsorbent surface is primarily influenced by the surface charge on the adsorbent. As zeolite particles exhibit negative charge in water, electrostatic interaction will favor the adsorption of Ni^{2+} ions on zeolite. In addition, the pore size of zeolite molecule could play a role in adsorption. Large size molecules will not easily penetrated into the inner pores of the adsorbent, resulting in lower adsorption capacity. The kinetics of adsorption can be described using several models.

3.3. Adsorption equilibrium

In the adsorption process of a solute from solution onto a solid surface, the solute adsorbed on the solid surface is in a dynamic equilibrium with the solute remained in solution. A plot of the solute concentration adsorbed on the solid surface (mg/g) as a function of the solute concentration in the solution at equilibrium (mg/L), at constant temperature, gives an adsorption isotherm, which can be described by some adsorption models [28,29]. Some isotherm equations have been tested in the present study, namely the Freundlich (Eq. 2) and Langmuir (Eq. 3) isotherm models:

$$q_e = K_F C_e^N \tag{2}$$

$$q_e = \frac{K_L b C_e}{1 + K_L C_e} \tag{3}$$

where q_e is the amount of metal ion adsorbed in mg/g; C_e is the concentration (mg/L) of metal ion in the solution at equilibrium; K_F, Freundlich constant which predicts the quantity of metal ion per gram of resin at the unit equilibrium concentration; N, a measure of the nature and strength of the adsorption process and of the distribution of active sites. If $N < 1$, bond energies increase with the surface density; if $N > 1$, bond energies decrease with the surface density; and when $N = 1$, all surface sites are equivalent. The Langmuir constants K_L and b represent adsorption equilibrium constant and saturated monolayer adsorption capacity, respectively.

The constants corresponding to the adsorption models were calculated with an Origin 8.1 program by applying Eq. (2) for the Freundlich model and Eq. (3) for the Langmuir model and were collected in Table 2.

As Table 2 shows, the experimental data obtained for the adsorption of Ni^{2+} ions onto Akdere zeolite was well-fitted in the Freundlich model with a maximum theoretical adsorption capacity of 3.56 mg Ni^{2+}/g Akdere zeolite. Akdere zeolite is favorable for adsorption of Ni^{2+} ions under the selected conditions (Table 3). In Table 4, several adsorbents are given for nickel adsorption. Even though, adsorption amount for other adsorbents seem higher than Akdere zeolite [29–35], considering the experiment conditions Akdere zeolite give the best results for nickel removal.

3.3.1. Pseudo-first-order model

$$\frac{dq_t}{dt} = k_1(q_e - q_t) \tag{4}$$

where k_1 is the rate constant of pseudo-first-order adsorption and q_e denotes the amount of adsorption at equilibrium. After definite integration by applying the initial conditions $q_t = 0$ at $t = 0$ and $q_t = q_t$ at $t = t$, Eq. (4) becomes

$$\ln(q_e - q_t) = \ln q_e - k_1 t \tag{5}$$

The above linear equation (Eq. 5) based on $\ln(q_e - q_t)$ and t can usually be used to estimate the equilibrium adsorption q_e (intercept) and rate constant k_1 (slope). If the calculated q_e from intercept is equal to the experimental q_e, it would suggest the adsorption following the first-order kinetics [10,15,27,35] (Fig. 10).

Table 2
Adsorption isotherm constants of Freundlich and Langmuir models for the adsorption of Ni(II) on Akdere zeolite

	Freundlich isotherm			Langmuir isotherm		
℃	K_F	$1/n$	R^2	K_L	b	R^2
25	5.261	0.487	0.990	3.789	1.708	0.982
45	5.403	0.446	0.971	3.902	1.903	0.961
75	5.804	0.412	0.993	4.187	2.685	0.964

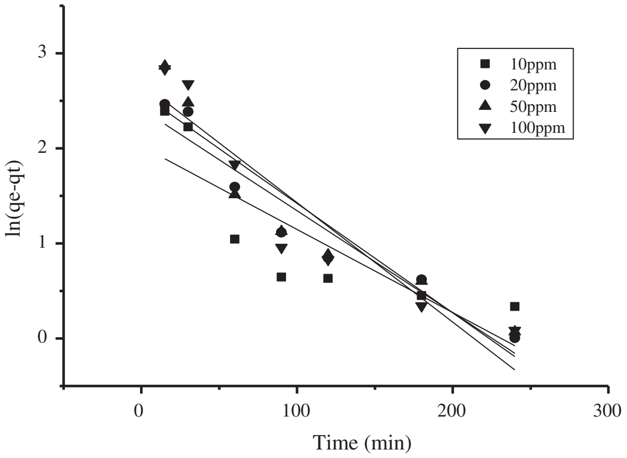

Fig. 10. The first-order kinetics of Ni^{2+} adsorption on Akdere zeolite.

3.3.2. Pseudo-second-order model

A pseudo-second-order equation based on adsorption equilibrium capacity may be expressed in the form (Eq. 6)

$$\frac{dq_t}{dt} = k_2(q_e - q_t)^2 \tag{6}$$

where k_2 is the rate constant of pseudo-second-order adsorption. Integrating and applying the initial conditions, we have a linear form as (Eq. 7) (Fig. 11)

$$\frac{t}{q_t} = \frac{1}{k_2 {q_e}^2} + \frac{1}{q_e} t \tag{7}$$

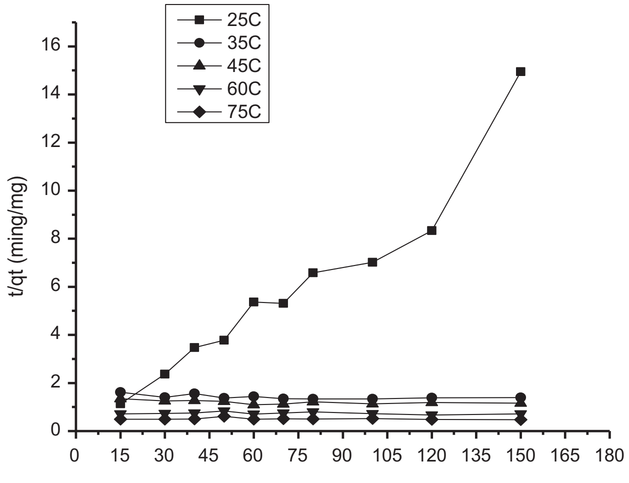

Fig. 11. The second-order kinetics of Ni^{2+} adsorption on Akdere zeolite.

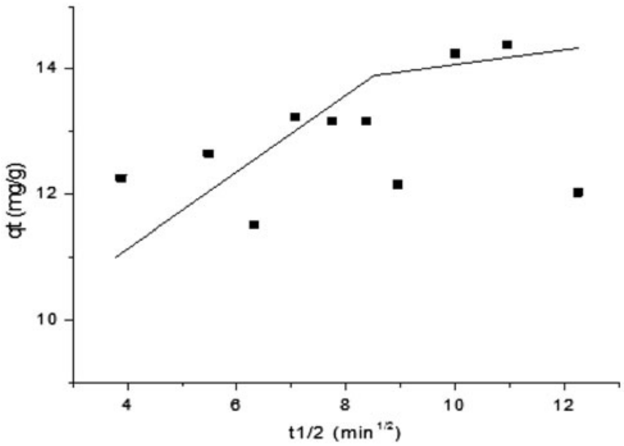

Fig. 12. Intraparticle diffusion model of Ni^{2+} adsorption on Akdere zeolite.

3.3.3. Intraparticle diffusion model

In addition, another simplified model, intraparticle diffusion model, is also tested. The initial rate of the intraparticle diffusion is the following:

$$q_t = k_p\left(t^{1/2}\right) \tag{8}$$

where k_p is the intraparticle diffusion rate constant.

Figs. 10 and 11 present the linear forms of the pseudo-first-order and pseudo-second-order kinetics of Ni^{2+} ions adsorbed on zeolite and the calculated kinetic parameters are given in Table 3. As seen, the pseudo-first-order kinetics curve does not show a straight line and two sections can be clearly identified. Comparing the adsorption equilibrium, it is seen that the value at 75°C are not so different from the value at 25°C, conformed to the experimental data.

Fig. 12 shows the diffusion modeling on kinetics of Ni^{2+} ions adsorption on zeolite. The results indicated that the adsorption process of Ni^{2+} ions exhibits two separate regions with two straight lines. The first straight portion is attributed to a macropores diffusion

Table 3
Kinetic models for the adsorption of Ni(II) onto Akdere zeolite

	Pseudo-first-order model			Pseudo-second-order model		
	k_1	q_e	R^2	k_2	q_e	R^2
25°C	0.034	3.46	0.891	0.934	5.27	0.913
45°C	0.041	3.61	0.866	1.109	5.12	0.957
75°C	0.047	5.99	0.973	1.305	6.75	0.981

Table 4
Adsorption of Ni(II) ions on various adsorbents

Adsorbent type	Maximum conditions	Adsorbed amount (mg/g)	Reference
NKF-6 zeolite	0.6 g/L, 9.222 mg/L, 250 ml, pH 6.25	17.40	[2]
Boron sludge	pH 7; 90 min; 2 g/L; 50 ml; 150 mg/L	69.13	[9]
Zeolite–attapulgite composite	20 mg/L; 2 h; pH 7; 12 g; 150 ml	80 g/L	[42]
Bentonite	100 mg/L; 0.6 g; 100 ml; 30 min	16.70	[43]
Chitosan–clin composite	0.25 g; 25 ml; 0.07 mol/L; pH 5	0.24	[7]
Natural zeolite	0.01 mol/L; 2 h; pH 4–6; 0.2 g; 20 ml	4.60	[6]
NH_4-zeolite	0.01 mol/L; 2 h; pH 4–6; 0.2 g; 20 ml	5.30	[6]
Na-zeolite	0.01 mol/L; 2 h; pH 4–6; 0.2 g; 20 ml	5.00	[6]
Granule active carbon	pH 5; 24 h; 20 mg/L	4.00	[5]
Natural zeolite	50 ml; 10 g; 1–12 h; 50 mg/L	0.247	[4]
Natural zeolite	pH 5; 50 ml; 5 mg/L; 1 g adsorbent	0.44	[41]
Natural zeolite	pH 5; 10 mg/L; 1 h; 0.1 g; 250 ml	3.56	In this study

Table 5
Thermodynamic parameters of Ni(II) adsorption on natural zeolite

ΔG° (kJ/mol)					ΔH° (kJ/mol)	ΔS° (J/mol K)
25℃	35℃	45℃	60℃	75℃		
−2.09	−3.09	−2.24	−0.56	0.43	21.08	60.94

process and the second linear portion can be ascribed to a micropores diffusion process. In addition, it is clear from Fig. 12 that the first stage is faster than the second one. This behavior may be correlated with the very slow diffusion of the adsorbate from the surface film into the micropores. Previous studies [3,27,28] have showed similar results that a multi-step is involved in the adsorption process of nickel on several solid adsorbents.

Based on the adsorption constant K_L in the Langmuir isotherm, thermodynamic parameters, i.e. free energy (ΔG°), enthalpy (ΔH°), and entropy (ΔS°), changes were also calculated using Eqs. (9)–(11) and are given in Table 2:

$$\Delta G^\circ = -RT \ln K_L \tag{9}$$

$$\Delta H^\circ = -R\left(\frac{T_2 T_1}{T_2 - T_1}\right) \ln \frac{K_{L1}}{K_{L2}} \tag{10}$$

$$\Delta S^\circ = \frac{\Delta H^\circ - \Delta G^\circ}{T} \tag{11}$$

In Table 5, adsorption process is spontaneous with the negative values of ΔG°. The standard enthalpy change (ΔH°) for the adsorption of two dyes on natural zeolite is positive indicating that the process is endothermic in nature. The positive value of ΔS° shows increased disorder at the solid–solution interface during the adsorption of Ni^{2+} ions. The adsorption increases randomness at the solid/solution interface with some structural changes in the adsorbate and adsorbent and an affinity of the adsorbent [36–40].

4. Conclusions

A novel zeolite (Akdere zeolite) was used for the removal of Ni^{2+}, as a function of different parameters like: pH, contact time, metal ion concentration, and temperature. The optimum adsorption pH of all metal ions was located at 7 and the contact time required to achieve the equilibrium was 60 min.

The adsorption process of Ni^{2+} ions obeyed of the pseudo-second-order kinetics, supporting the chemisorption would be the rate-determining step. The equilibrium data obtained for the adsorption of all metal ions onto Akdere zeolite well fitted in the Freundlich model with a maximum theoretical adsorption capacity of 3.56 mg Ni^{2+}/g zeolite. The adsorption process was spontaneous (ΔG°ads <0) and endothermic (ΔH°ads >0), supporting also the chemisorption is the rate-determining step. The intraparticle diffusion results pointed to the presence of macropores in the first stage and micropores as a second stage of the adsorption process.

The results showed that Akdere natural and modified zeolite has higher adsorption capacity than other zeolites found in Turkey. It is really a low-cost material for nickel removal from aqueous solutions.

References

[1] N.T. Abdel-Ghani, G.A. El-Chaghaby, F.S. Helal, Individual and competitive adsorption of phenol and nickel onto multiwalled carbon nanotubes, J. Adv. Res. (In press), doi: 10.1016/j.jare.2014.06.001.

[2] H. Zhang, X. Yu, L. Chen, Y. Jing, Z. Ge, Study of ^{63}Ni adsorption on NKF-6 zeolite, J. Environ. Radioact. 101 (2010) 1061–1069.

[3] M. Çanlı, Y. Abalı, S.U. Bayça, Removal of methylene blue by natural and Ca and K-exchanged zeolite treated with hydrogen peroxide, Physicochem. Probl. Miner. Process. 49(2) (2013) 481–496.

[4] R.A. Al Dwairi, A.E. Al-Rawajfeh, Removal of Cobalt and Nickel from wastewater by using Jordan Low-cost zeolite and bentonite, J. Univ. Chem. Technol. Metall. 47(1) (2012) 69–76.

[5] F. Tümsek, B. Karabacakoğlu, Ni(II) İyonlarının Sulu Çözeltiden Granül Aktif Karbon Üzerine Adsorpsiyonu (Ni(II) Ions Adsorption onto Granular Activated Carbon from Aqueous Solutions). III. Fiziksel Kimya Günleri (Physical Chemistry Days), July 12–15, Burhaniye, Balıkesir, Turkey, 2012.

[6] M. Çanlı, Modification of zeolite and examining its surface properties, Unpublished Ph.D. Thesis, Celal Bayar University Institute of Science and Technology, 2013.

[7] M.V. Dinu, E.S. Dragan, Evaluation of Cu^{2+}, Co^{2+} and Ni^{2+} ions removal from aqueous solution using a novel chitosan/clinoptilolite composite: Kinetics and isotherms, Chem. Eng. J. 160 (2010) 157–163.

[8] I. Rodríguez-Iznaga, A. Gómez, G. Rodríguez-Fuentes, A. Benítez-Aguilar, J. Serrano-Ballan, Natural clinoptilolite as an exchanger of Ni^{2+} and NH_4^+ ions under hydrothermal conditions and high ammonia concentration, Microporous Mesoporous Mater. 53 (2002) 71–80.

[9] A. Ates, C. Hardacre, The effect of various treatment conditions on natural zeolites: Ion exchange, acidic, thermal and steam treatments, J. Colloid Interface Sci. 372 (2012) 130–140.

[10] A. Malekpour, M. Edrisi, S. Hajialigol, S. Shirzadi, Solid phase extraction–inductively coupled plasma spectrometry for adsorption of Co(II) and Ni(II) from radioactive wastewaters by natural and modified zeolites, J. Radioanal. Nucl. Chem. 288 (2011) 663–669.

[11] F. Cakicioglu-Ozkan, S. Ulku, The effect of HCl treatment on water vapor adsorption characteristics of clinoptilolite rich natural zeolite, Microporous Mesoporous Mater. 77 (2005) 47–53.

[12] B. Erdoğan, M. Sakızcı, E. Yörükoğulları, Characterization and ethylene adsorption of natural and modified clinoptilolites, Appl. Surf. Sci. 254 (2008) 2450–2457.

[13] P. Chutia, S. Kato, Adsorption of As(V) on surfactant-modified natural zeolites, J. Hazard. Mater. 162 (2009) 204–211.

[14] D. Woumfo, R. Kamga, F. Figueras, D. Njopwouo, Acid activation and bleaching capacity of some Cameroonian smectite soil clays, Appl. Clay Sci. 37 (2007) 149–156.

[15] E. Yerlikaya, Removal of Nickel (II) and Lead (II) by adsorption method from wastewaters, Unpublished Master Thesis, Institute of Science at Dumlupınar University, 2008.

[16] W. Mozgawa, The influence of some heavy metals cations on the FTIR spectra of zeolites, J. Mol. Struct. 555 (2000) 299–304.

[17] T. Ünaldı, Ö. Orhun, S. Kadir, Physicochemical characterization of natural and Na^+-, K^+-, Ca^{2+}- and Mg^{2+}-modified clinoptilolite from Gördes (Manisa, Turkey), Adsorpt. Sci. Technol. 27(6) (2009) 615–631.

[18] X. Wang, O. Ozdemir, M.A. Hampton, A.V. Nguyen, D.D. Do, The effect of zeolite treatment by acids on sodium adsorption ratio of coal seam gas water, Water Res. 46 (2012) 5247–5254.

[19] V.K. Jha, S. Hayashi, Modification on natural clinoptilolite zeolite for its NH_4^+ retention capacity, J. Hazard. Mater. 169 (2009) 29–35.

[20] S.R. Taffarel, J. Rubio, On the removal of Mn^{2+} ions by adsorption onto natural and activated Chilean zeolites, Miner. Eng. 22(4) (2009) 336–343.

[21] U. Wingenfelder, B. Nowack, G. Furrer, R. Schulin, Adsorption of Pb and Cd by amine-modified zeolite, Water Res. 39 (2005) 3287–3297.

[22] Y. Akdeniz, Cation exchange in zeolites, structural modification by using a microwave, Unpublished Master Thesis, Izmir Institute of Technology, 1999.

[23] M. Sakızcı, E. Yörükoğulları, Gördes yöresi klinoptilolitinin (doğal ve modifiye) su buharı adsorpsiyonu (Water vapor adsorption on natural and modified forms of Gördes zeolite), Eskisehir. Osmangazi. Univ. J. Eng. Arch. XX(1) (2007) 33–46.

[24] S. Yetgin, Investigation of fuel oxygenate adsorption on clinoptilolite rich natural zeolite, Unpublished Master Thesis, The Graduate School of Engineering and Science of Izmir Institute of Technology, 2006.

[25] M.G. Macedo-Miranda, M.T. Olguín, Arsenic sorption by modified clinoptilolite–heulandite rich tuffs, J. Inclusion Phenom. Macrocyclic Chem. 59 (2007) 131–142.

[26] J. Torres-Pérez, M. Solache-Ríos, M.T. Olguín, Sorption of azo dyes onto a Mexican surfactant-modified clinoptilolite-rich tuff, Sep. Sci. Technol. 42 (2007) 299–318.

[27] M.G.A. Vieira, A.F.A. Neto, M.L. Gimenes, M.G.C. da Silva, Removal of nickel on Bofe bentonite calcined clay in porous bed, J. Hazard. Mater. 176 (2010) 109–118.

[28] P. Panneerselvam, V.S.S. Bala, N. Thinakaran, P. Baskaralingam, M. Palanichamy, S. Sivanesan, Removal of Nickel(II) from aqueous solutions by adsorption with modified ZSM-5 zeolites, Electron-J. Chem. 6(3) (2009) 729–736.

[29] T. Motsi, N.A. Rowson, M.J.H. Simmons, Adsorption of heavy metals from acid mine drainage by natural zeolite, Int. J. Miner. Process. 92 (2009) 42–48.

[30] N. Halimoon, R.G.S. Yin, Removal of heavy metals from textile wastewater using zeolite, Environment Asia, 3 (2010) (Special issue), 124–130.

[31] Ö. Can, D. Balköse, S. Ülkü, Batch and column studies on heavy metal removal using a local zeolitic tuff, Desalination 259 (2010) 17–21.

[32] S. Kocaoba, Y. Orhan, T. Akyüz, Kinetics and equilibrium studies of heavy metal ions removal by use of natural zeolite, Desalination 214 (2007) 1–10.

[33] S. Wang, Y. Peng, Natural zeolites as effective adsorbents in water and wastewater treatment, Chem. Eng. J. 156 (2010) 11–24.

[34] K.S. Hui, C.Y.H. Chao, S.C. Kot, Removal of mixed heavy metal ions in wastewater by zeolite 4A and residual products from recycled coal fly ash, J. Hazard. Mater. 127 (2005) 89–101.

[35] M. Uğurlu, I. Kula, M.H. Karaoğlu, Y. Arslan, Removal of Ni(II) ions from aqueous solutions using activated-carbon prepared from olive stone by $ZnCl_2$ activation, Environ. Prog. Sustain Energy 28(4) (2009) 547–557.

[36] M. Uğurlu, M. Sarioglu, S. Akkoyun, T. Bisgin, Inhibition effects of heavy metals (copper, nickel, zinc, lead) on anaerobic sludge, Desalin. Water Treat. 23 (2010) 55–60.

[37] T. Ünaldı, B. Yıldırım, Gördes yöresi doğal zeolitinin NH_4^+ formlarının incelenmesi (Examination of NH_4^+ forms of Gördes natural zeolites), Anadolu Univ. J. Sci. Technol. 10(2) (2009) 485–493.

[38] M. Sarioglu, Removal of ammonium from municipal wastewater using natural Turkish (Dogantepe) zeolite, Sep. Purif. Technol. 41 (2005) 1–11.

[39] S. Çoruh, G. Şenel, O.N. Ergun, A comparison of the properties of natural clinoptilolites ve their ion-exchange capacities for silver removal, J. Hazard. Mater. 180 (2010) 486–492.

[40] T. Ünaldı, CO2 adsorption of ion exchange forms of natural zeolite from Bigadiç region, Unpublished Ph.D. Thesis, Osmangazi University Institute of Science and Technology Physics Department, 1995.

[41] E. Aras, Adsorption of Ni (II) from water, Unpublished Master Thesis, Celal Bayar University Institute of Science and Technology, 2010.

[42] W. Zheng, Z. Lin-sheng, J. Zhao-qian, Adsorption of nickel ion by zeolite-attapulgite composite nano-size adsorbent, 3rd International Conference on Bioinformatics and Biomedical Engineering (ICBBE), June 11–13, 2009, Beijing, China.

[43] T. Çevik, S. Top, E. Sekman, R. Yazıcı, M.S. Bilgili, A. Demir, G. Varank, E. Akkaya, Nikelin Bentonitle Adsorpsiyonunun İzoterm, Kinetik ve Termodinamik Analizi, Üniversite Öğrencileri, III. Çevre Sorunları Kongresi (ÇESKO) (Isothermal, Kinetic and Thermodynamical Analysis of Nickel adsorption onto Bentonite, III Congress on Environmental problems), Istanbul, Turkey, May 16–18, 2008.